

THE DENSITY OF LY α EMITTERS AT VERY HIGH REDSHIFT

ESTHER M. HU¹ AND LENNOX L. COWIE¹

Institute for Astronomy, University of Hawaii, 2680 Woodlawn Drive, Honolulu, HI 96822
hu@ifa.hawaii.edu, cowie@ifa.hawaii.edu

AND

RICHARD G. McMAHON¹

Institute of Astronomy, University of Cambridge, Madingley Road, Cambridge CB30HA
rgm@ast.cam.ac.uk

Draft version March 1, 1998

ABSTRACT

We describe narrowband and spectroscopic searches for emission-line star forming galaxies in the redshift range 3 – 6 with the 10 m Keck II Telescope. These searches yield a substantial population of objects with only a single strong (equivalent width $\gg 100 \text{ \AA}$) emission line, lying in the 4000 – 8500 \AA range. Spectra of the objects found in narrowband-selected samples at $\lambda \sim 5390 \text{ \AA}$ and $\sim 6741 \text{ \AA}$ show that these very high equivalent width emission lines are generally redshifted Ly α $\lambda 1216 \text{ \AA}$ at $z \sim 3.4$ and 4.5. The density of these emitters above the 5σ detection limit of $1.5 \times 10^{-17} \text{ ergs cm}^{-2} \text{ s}^{-1}$ is roughly $15,000/\square^\circ/\text{unit } z$ at both $z \sim 3.4$ and 4.5. A complementary deeper ($1 \sigma \sim 10^{-18} \text{ ergs cm}^{-2} \text{ s}^{-1}$) slit spectroscopic search covering a wide redshift range but a more limited spatial area ($200 \square''$) shows such objects can be found over the redshift range $z = 3 - 6$, with the currently highest redshift detected being at $z = 5.64$. The Ly α flux distribution can be used to estimate a minimum star formation rate in the absence of reddening of roughly $0.01 M_\odot \text{ Mpc}^{-3} \text{ yr}^{-1}$ ($H_0 = 65 \text{ km s}^{-1} \text{ Mpc}^{-1}$, $q_0 = 0.5$). Corrections for reddening are likely to be no larger than a factor of two, since observed equivalent widths are close to the maximum values obtainable from ionization by a massive star population. Within the still significant uncertainties, the star formation rate from the Ly α -selected sample is comparable to that of the color-break-selected samples at $z \sim 3$, but may represent an increasing fraction of the total rates at higher redshifts. This higher- z population can be readily studied with large ground-based telescopes.

Subject headings: cosmology: observations — early universe — galaxies: evolution — galaxies: formation

1. INTRODUCTION

The search for high-redshift galaxies and the effort to map the star formation history of galaxies have progressed rapidly in the last several years as magnitude-limited spectroscopic surveys pushed into the $z = 1 - 3$ range (Cowie et al. 1996; Cohen et al. 1996), while color-based selection techniques produced many objects in the $z = 2.5 - 5$ range (Steidel et al. 1996a, 1996b; Franx et al. 1997; Steidel et al. 1998), particularly in the exquisite Hubble Deep Field (HDF) sample (Lowenthal et al. 1997). However, the galaxies chosen by these techniques correspond to objects with ongoing massive star formation and small amounts of extinction, and may represent only part of the populations at these early epochs. More evolved objects may be heavily dust-reddened and more easily picked out at submillimeter wavelengths (Smail, Ivison, & Blaine 1997; Hauser et al. 1998), while earlier stages in evolution may have relatively little continuum light and be too faint to be seen in the magnitude-limited samples or selected with the color-break techniques at current sensitivity limits.

This latter class of objects may represent the earliest stages of the galaxy formation process, in which substantial amounts of metals have yet to form. These galaxies may have much stronger Ly α emission relative to the stellar continuum, since they have massive star formation that

can excite the Ly α emission line, but without so much dust that the line is suppressed, and this can result in very high observed equivalent widths in the range of 100–200 $(1+z) \text{ \AA}$ (e.g., Charlot & Fall 1993). Such objects may be hard to pick out with color-break techniques but be detectable in Ly α searches of sufficient depth (Cowie 1988; Thommes 1996). An increased incidence of strong Ly α emission does, indeed, appear in the color-break samples at fainter continuum magnitudes (Steidel et al. 1998).

Earlier blank-field Ly α surveys (e.g., Thompson, Djorgovski, & Trauger 1995; Thompson & Djorgovski 1995) failed to find such objects, as Pritchet (1994) has summarized, but their sensitivity lay at the margin of where such objects would be expected in significant numbers (Cowie 1988; Thommes & Meisenheimer 1995). However, Hu & McMahon (1996), using very deep targeted narrowband searches ($1 \sigma = 1.5 \times 10^{-18} \text{ ergs cm}^{-2} \text{ s}^{-1}$), found $z \sim 4.55$ Ly α -emitting galaxies with the very strong emission and weak or undetected continua predicted for early star-forming objects. The advent of 10 m telescopes, along with this successful detection of Ly α emitters, prompted us to undertake a new survey that has been successful in detecting blank-field high- z Ly α emitters. The present Letter describes the early results of this search, which uses extremely deep narrowband filter exposures taken with LRIS (Oke et al. 1995) on the Keck II telescope to search

¹Visiting Astronomer, W. M. Keck Observatory, jointly operated by the California Institute of Technology, the University of California, and the National Aeronautics and Space Administration.

for emission-line populations at extremely faint flux levels ($1\sigma = 3 \times 10^{-18}$ ergs cm^{-2} s^{-1}). This survey picks out sources of extremely high equivalent width ($W_\lambda > 100 \text{ \AA}$) emission lines as candidates, and then uses followup LRIS spectroscopy (§2) to determine if these are $\text{Ly}\alpha$ emitters.

The first results from the Hawaii survey with a 5390/77 \AA filter, corresponding to $\text{Ly}\alpha$ emission at $z \sim 3.4$, were described in Cowie & Hu 1998 (hereafter, Paper I), and yielded a number of candidate high- z galaxies similar to the redshift $z \sim 4.55$ $\text{Ly}\alpha$ -emitting galaxies found by Hu & McMahon (1996) and emitters at $z \sim 2.4$ (Pascarelle et al. 1996; Francis et al. 1997) in targeted searches. In Paper I, we showed that the use of color selection on emission-line selected objects of high equivalent width ($> 100 \text{ \AA}$) picked out objects with continuum colors similar to those of color-selected Lyman break galaxies with measured redshifts of $z \sim 3.4$. They also recovered the one field object whose previously measured redshift placed $\text{Ly}\alpha$ within the filter bandpass. However, the emission-line galaxies selected by their high equivalent width also comprised objects with very faint continua, that would have fallen below the magnitude threshold of current Lyman break surveys, and also included two objects that could not be detected in Keck imaging of the optical continuum ($1\sigma B = 27.8$, $V = 27.5$, and $I = 25.8$; $W_\lambda > 400 \text{ \AA}$).

In the present Letter we first present spectroscopic followups for the narrowband candidates of Paper I. In a small fraction of the cases, the spectrum shows both $\text{Ly}\alpha$ and $\text{CIV } \lambda 1550 \text{ \AA}$, confirming the redshift identification but suggesting AGN-like properties. However, the majority of the spectra show only a single strong emission line. The absence of other detectable features, in combination with the high equivalent width of the selected candidates, identifies the single line as redshifted $\text{Ly}\alpha$ emission, and argues that the equivalent width criterion ($W_\lambda \gg 100 \text{ \AA}$) can, in fact, be used as a good diagnostic of high- z $\text{Ly}\alpha$ -emitting galaxies. We then (§3) present results of a second deep narrowband search with a 78 \AA bandpass $\lambda \sim 6741 \text{ \AA}$ filter ($\text{Ly}\alpha$ at $z \sim 4.54$) and followup spectroscopy, that confirmed two $\text{Ly}\alpha$ -emitting galaxies at this higher redshift. In §4, we describe a very deep blank-field spectroscopic search (6 hr LRIS integration covering $\lambda \sim 5000 - 10000 \text{ \AA}$) that yielded four emitters at redshifts 3.04 – 5.64. Finally (§5), the data on emission-line objects from the imaging surveys in the two redshift intervals are combined with various spectroscopic surveys at lower redshift to show the evolution of the emission-line fluxes with redshift. We argue that the $\text{Ly}\alpha$ -emitting objects are significant contributors to the integrated star formation of the galaxy population throughout the $z = 3 - 6$ redshift range, and that the integrated star formation rate of the $\text{Ly}\alpha$ selected objects is flat, or possibly rising through this redshift range, with a value greater than $0.01 M_\odot \text{ Mpc}^{-3}$ for $q_0 = 0.5$ and $H_0 = 65 \text{ km s}^{-1} \text{ Mpc}^{-1}$. At the highest redshifts, most of the star formation may be occurring in objects of this class.

2. SPECTROSCOPIC CONFIRMATION OF CANDIDATE LYMAN ALPHA EMITTERS

Paper I provides a sample of 12 objects in the SSA22 and HDF fields, with $W_\lambda > 100 \text{ \AA}$ in the 5390/77 \AA filter. A

further 7 objects were detected in a similar field surrounding the $z \sim 4.53$ quasar BR0019–1522 (Storrie-Lombardi et al. 1996), giving a total sample of 19 objects over an area of $75 \text{ \square}'$. All the SSA22 and HDF candidate objects have now been spectroscopically observed using LRIS on the Keck II telescope, as have three of the objects in the BR0019–1522 field. Multi-slit masks with $1''4$ slits were used, giving a resolution of 16 \AA (Cowie et al. 1996), and exposure times ranged from 1 – 3 hrs, with most objects having the longer exposure. Two objects in the HDF field have strong CIV emission, placing them at $z = 3.40$ but suggesting AGN activity (Fig. 1). These objects appear similar to the brighter objects in Pascarelle et al. (1996). However, the remaining objects have only one strong emission line, and the continua are too weak for absorption line identifications.

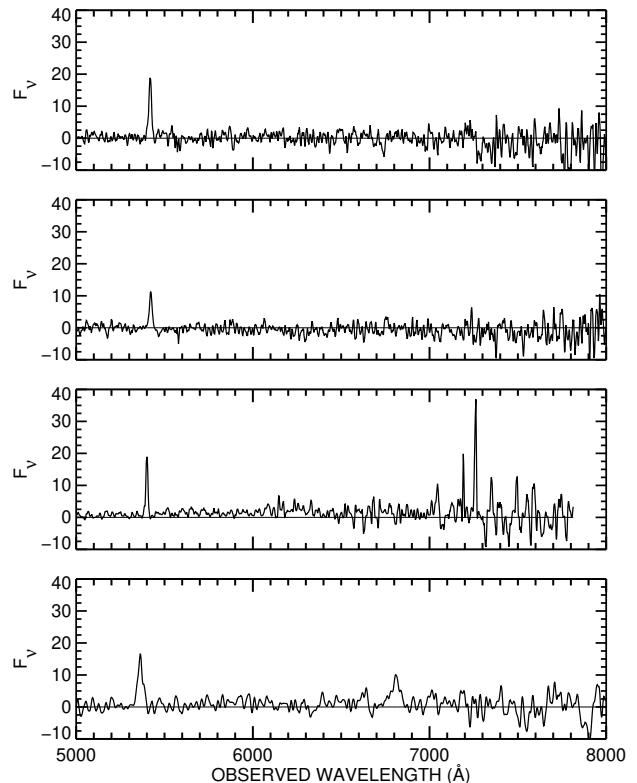


Figure 1. Spectra of strong $\text{Ly}\alpha$ emitters in SSA22, LA1 and LA3, (top two panels) compared with the spectrum of an $[\text{O II}]$ emitter with extremely high equivalent width (third panel) shifted so the $[\text{O II}]$ emission lies at the narrowband wavelength (5390 \AA). We also show for comparison one of the two $\text{Ly}\alpha$ emitters (LA1) in the HDF field that shows strong CIV emission (bottom panel). The observed equivalent widths of the two SSA22 objects are 325 \AA for the topmost object and $> 800 \text{ \AA}$ for the second. The observed equivalent width of the $[\text{O II}]$ line in the comparison object is 220 \AA . The $\text{H}\beta + [\text{O III}]$ complex is clearly evident in the case of the $[\text{O II}]$ emitter, and these cases may be easily distinguished from genuine high- z $\text{Ly}\alpha$ emission objects.

A primary concern in the simple equivalent width selection procedure is whether we are misinterpreting emission lines such as $[\text{O II}] 3727 \text{ \AA}$ and $\text{H}\alpha 6563 \text{ \AA}$, that are common features in galaxies at moderate redshift, as higher redshift $\text{Ly}\alpha$ emission. For objects where the continuum is strongly detected it is possible to use color information to diagnose the different lines (Paper I), but in cases in which only one emission line is seen, we can only make the distinction based on the equivalent width strength of the line, assuming that an observed equivalent width $W_\lambda \gg 100 \text{ \AA}$ is generally $\text{Ly}\alpha$ rather than unusually strong $[\text{O II}]$ or

$H\alpha$. Spectroscopic followup is therefore essential to decide whether this procedure is reliable.

It is easiest to argue that single-line objects are $Ly\alpha$ emitters at lower redshifts, where the number of possible contaminating lines is smaller. An emission line at 5390 Å lies below rest-frame $H\alpha$, and only slightly above the [O III]+ $H\beta$ complex at 5000 Å, so that the only probable sources of confusion are [O II] 3727 emitters at $z = 0.45$. However, such objects would then have $H\beta$ 4861 and [O III] 5007 lying at 7030 Å and 7241 Å, and we would expect these emission lines to be strong, given the necessary strength of the [O II] 3727 line. In Figure 1 we compare the spectra of two strong emitters ($W_\lambda = 325$ and > 845 Å) found in the SSA22 field with one of the strongest equivalent width [O II] emitters ($W_\lambda = 220$ Å) found in the Hawaii Deep Field Survey of Cowie et al. (1996), and with one of the objects with $Ly\alpha$ and C IV emission detected in the HDF. The [O II] comparison spectrum has been wavelength shifted so that its [O II] line lies over the emission lines in the objects. It can be clearly seen that the absence of the $H\beta$ + [O III] complex in the SSA22 spectra rules out the possibility that the objects are [O II] emitters, and leaves us only with the $Ly\alpha$ interpretation.

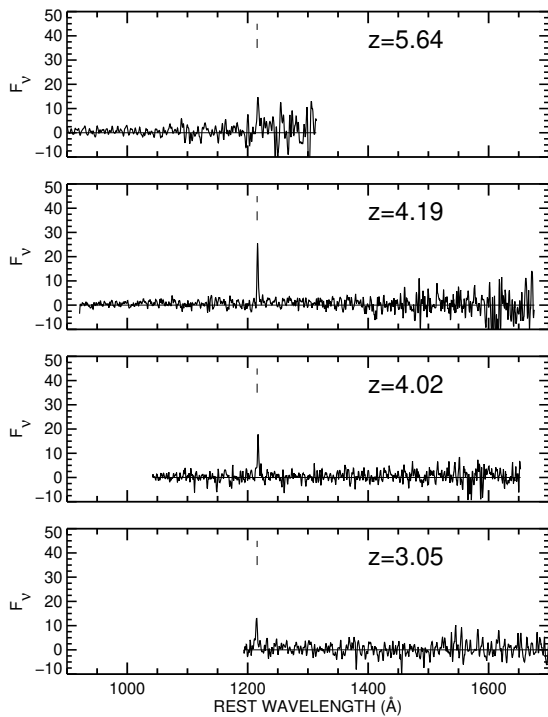


Figure 4. The plots show $Ly\alpha$ emission-line objects recovered from deep multi-slit spectroscopy of a field around the quasar BR1202–0725 using LRIS. The 4 detected objects have observed equivalent widths of > 600 , > 600 , 450, and 350 Å. See Fig. 3 for the corresponding two-dimensional spectra. If the emission line were [O II], the $H\beta$ + [O III] complex would lie in the 1600 – 1630 Å region.

3. LYMAN ALPHA EMITTERS AT $Z = 4.52$

Narrowband observations of the SSA22 field were obtained on the nights of UT 1997 September 21–22 with the LRIS camera on Keck II, through a narrowband interference filter centered at 6741 Å, with a bandpass of 78 Å and transmission of 81%. The net exposure of 2.7 hrs was obtained as a sequence of 900 s exposures taken with $10''$ offsets, with FWHMs of $0''.85$ (1.2 hrs) and $0''.65$ (1.5

hrs). A corresponding 1.2 hr R -band image was obtained as a series of 360 s exposures to define the local continuum. Three $W_\lambda > 100$ Å objects were detected, which are marked on the narrowband image in Figure 2 (Plate 1), and shown as 2-dimensional spectra in Figure 3 (Plate 2).

At this narrowband wavelength (6741 Å) we may be contaminated by [O II] 3727 at $z = 0.8$, $H\alpha$ at $z = 0.03$, or [O III] or $H\beta$ at $z \sim 0.37$. However, our spectroscopic followup again easily distinguishes such cases. The lowest flux object, with the weakest equivalent width constraint ($W_\lambda = 120$ Å), is identified as an [O II] emitter at $z = 0.814$, but the stronger object with substantial red wavelength coverage does not have detected [O III] and does not permit this interpretation. For the second strong object there is a strong break across the emission line, consistent with the $Ly\alpha$ interpretation. Nor does either of the objects have emission lines near the primary line, that would permit the objects to be identified as [O III] or $H\beta$. Once again there appears no choice but to interpret these lines as $Ly\alpha$.

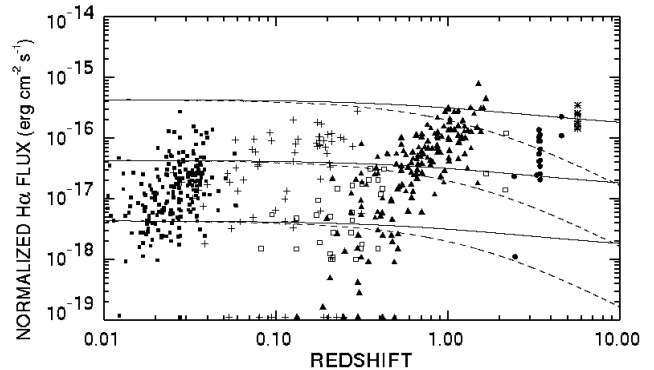


Figure 5. Composite plot of $H\alpha$ flux times redshift squared versus redshift. At low redshift we show the $f(H\alpha + [N II]) \times z^2$ fluxes (filled squares) from the $z \lesssim 0.045$ sample of Gallego et al. (1995), converted to corresponding $H\alpha$ flux by multiplying by 0.75. The crosses show normalized $H\alpha$ fluxes or converted, normalized [O II] fluxes from the Hawaii wide-field surveys (Songaila et al. 1994). The filled triangles show renormalized, converted [O II] fluxes from a $B = 25$ spectroscopic sample (cf., Cowie et al. 1997) with open squares showing renormalized $f(H\alpha + [N II]) \times z^2$ or with circles showing renormalized $f(Ly\alpha)$ at the highest redshifts if the spectrum does not cover [O II]. Finally, the remaining circles (at $z \sim 3.43$ and $z \sim 4.54$ show $f(Ly\alpha) \times z^2 / 8.7$ for the samples of objects detected in the two narrowband filters. The asterisks show the corresponding CADIS data of Thommes et al. 1998. The solid ($q_0 = 0.5$) and dashed ($q_0 = 0.02$) reference lines show the fluxes corresponding to star formation rates $\dot{M} = 10, 1,$ and $0.1 M_\odot \text{ yr}^{-1}$ for $H_0 = 65 \text{ km s}^{-1} \text{ Mpc}^{-1}$ and the \dot{M} normalization discussed in the text.

4. SPECTROSCOPIC SEARCH

The surface density of emitters from the narrowband search is sufficiently high ($\sim 15,000/\Omega^2/\text{unit } z$ at $z = 3.4$, based on the 3 fields) that searches of existing very deep long-slit or multi-slit LRIS observations should yield such objects over the optical redshift range ($z \sim 2 - 7$). Indeed, Franx et al. 1997 identified a second $z \sim 4.92$ object by inferring that the single strong emission line seen in a serendipitously placed slit during spectroscopic exposures of their color-selected, gravitationally lensed galaxy, was also due to $Ly\alpha$ at their target object's redshift. In our own archival LRIS data the best suited exposure is that around the quasar BR1202–0725, where a 6 hr integration in a single mask configuration was obtained under photometric conditions and with reasonable seeing (UT 31 March – 2 April 1997; 4 hrs obtained with $0''.8 - 0''.85$

FWHM, and the remaining 2 hrs with $\sim 0''.95$ FWHM). The data were taken to study color-selected and emission-line-selected objects in the quasar field (Hu, McMahon, & Egami 1996; Giallongo et al. 1998) and the mask comprised only twelve slits, with the blank sky area covering roughly 200 arcsec². A search of this spectral image yielded four extremely high equivalent width emitters ranging in redshift from $z = 3.04 - 5.64$. These spectra are shown in Fig. 4 and in Plate 2. The two highest redshift objects can be seen in the red continuum, and have a strong break across the emission line, consistent with the expected Ly α forest decrement.

The surface density of emitters in the spectroscopic field is roughly 60,000 deg⁻²/unit z in the accessible redshift range, consistent with the narrowband searches when account is made for the slightly fainter flux limit in the spectroscopic data ($1 \sigma \sim 10^{-18}$ ergs cm⁻² s⁻¹) and the current uncertainty in the numbers. Ultimately, the census of the populations is best done with the narrowband data with its uniform selection procedures and well-defined flux limits, but the present data suggest that we will see substantial populations of these objects to very high redshift.

5. DISCUSSION

Since resonant scattering enhances the effects of extinction, it is harder to convert the Ly α emission into a massive star formation rate than it is for line luminosity diagnostics such as H α and [O II] 3727. For the present calculation, we assume that extinction may be neglected in computing the required massive star formation rates, which then constitute a minimum estimate. However, upward corrections to this value are unlikely to be larger than a factor of two, since the observed rest-frame equivalent widths lie in the 100 – 200 Å range — close to the maximum values that are obtainable from ionization by a massive star population (Charlot & Fall 1993). Then, assuming case B recombination, we have $L(\text{Ly}\alpha) = 8.7 L(\text{H}\alpha)$ (Brocklehurst 1971), which using Kennicutt's (1983) translation of \dot{M} from H α luminosity, gives $\dot{M} = (L(\text{Ly}\alpha)/10^{42} \text{ ergs s}^{-1}) M_{\odot} \text{ yr}^{-1}$. In order to cross-calibrate to [O II] fluxes at lower redshift we assume $f(\text{H}\alpha + [\text{N II}]) = 1.25 f([\text{O II}])$ based on the mean values of the ratio in both the Gallego et al. (1995) and Hawaii Deep Survey (Cowie et al. 1996) samples. We also assume $f(\text{H}\alpha + [\text{N II}]) = 1.33 f(\text{H}\alpha)$ (Kennicutt 1983).

In Figure 5 we compare the range of Ly α luminosities to the range of line luminosities in lower redshift objects. The plot shows the quantity $z^2 f$ vs redshift, where H $\alpha + [\text{N II}]$, [O II], and Ly α fluxes have been converted to H α fluxes

using the relationships above, and we have restricted ourselves to the imaging data in which the fluxes of the Ly α are well determined. The comparison objects are drawn from the surveys of Gallego et al. 1995 (*filled boxes*), Songaila et al. 1994 (*pluses*), and the Hawaii $B = 25$ sample [*open boxes* (H $\alpha + [\text{N II}]$), *triangles* ([O II]), and *circles* (Ly α)]. The CADIS candidate Ly α sample for $z = 5.7$ (Thommes et al. 1998) is shown with asterisks. The solid ($q_0 = 0.5$) and dashed ($q_0 = 0.02$) lines on Fig. 5 show the fluxes corresponding to stellar mass production rates of $10 M_{\odot} \text{ yr}^{-1}$, $1 M_{\odot} \text{ yr}^{-1}$, and $0.1 M_{\odot} \text{ yr}^{-1}$ for $H_0 = 65 \text{ km s}^{-1} \text{ Mpc}^{-1}$. Maximum formation rates locally are around a few $M_{\odot} \text{ yr}^{-1}$, rising to values of just over $10 M_{\odot} \text{ yr}^{-1}$ above $z = 0.6$. The Ly α fluxes at the higher redshifts are then consistent with this value or just slightly smaller depending on the extinction correction. The CADIS results lie a factor of several times higher in flux than the two Hawaii filter samples, which may suggest that the fluxes are rising to higher redshift. However, this result should be treated with great caution, since there may be substantial contamination by lower redshift emitters in the CADIS sample, and Thommes et al. 1998 estimate that statistically about half may be foreground.

The integrated star formation rates at $z = 3.4$ and $z = 4.5$ are $0.006 M_{\odot} \text{ Mpc}^{-3} \text{ yr}^{-1}$ and $0.01 M_{\odot} \text{ Mpc}^{-3} \text{ yr}^{-1}$ respectively for $q_0 = 0.5$ where the first value is slightly smaller than that given in Paper I since AGN-like objects are excluded. Both values are lower limits in the absence of extinction and the $z = 4.5$ value is based on a single field. The value inferred at $z = 5.7$ would be several times higher if all the CADIS objects are Ly α emitters. In combination, the results suggest that the star formation rates are constant or possibly increasing with redshift from $z = 3 - 6$, in contrast to color-based samples where the rate is declining at higher redshifts (Madau et al. 1996, 1997). This is consistent with the broad expectation that as we move to higher redshifts and earlier stages of galaxy formation, an increasingly larger fraction of the star formation should be in strong Ly α emitters that correspond to the youngest galaxies.

We thank T. Bida, R. Goodrich, J. Aycock, R. Quick, and W. Wack for their assistance in obtaining the observations. This work was supported by the State of Hawaii and by NASA grants GO-5975.01-94A, GO-6222.01-95A, and AR-6377.06-94A from Space Telescope Science Institute, which is operated by AURA, Inc., under NASA contract NAS 5-26555. E.M.H. acknowledges a University Research Council Seed Money grant. R.G.M. thanks the Royal Society for support.

REFERENCES

- Brocklehurst, M. 1971, MNRAS, 153, 471
 Charlot, S., & Fall, S. M. 1993, ApJ, 415, 580
 Cohen, J. G., Cowie, L. L., Hogg, D. W., Songaila, A., Blandford, R., Hu, E. M., & Shopbell, P. 1996, ApJ, 471, L5, astro-ph/9608121
 Cowie, L. L. 1988, in The Post-Recombination Universe, ed. N. Kaiser & A. N. Lazenby (Dordrecht: Kluwer), 1
 Cowie, L. L. & Hu, E. M. 1998, AJ, in press, (Paper I), astro-ph/9801003
 Cowie, L. L., Hu, E. M., Songaila, A., & Egami, E. 1997, ApJ, 481, L9, astro-ph/9702235
 Cowie, L. L., Songaila, A., Hu, E. M., & Cohen, J. G. 1996, AJ, 112, 839, astro-ph/9606079
 Fontana, A., Cristiani, S., D'Odorico, S., Giallongo, E., & Savaglio, S. 1996, MNRAS, 279, L27, astro-ph/9601086
 Francis, P. J., Woodgate, B. E., & Danks, A. C. 1997, ApJ, 482, L25, astro-ph/9703178
 Franx, M., Illingworth, G. D., Kelson, D. D., van Dokkum, P. G., & Tran, K.-V. 1997, ApJ, 486, L75, astro-ph/9704090
 Gallego, J., Zamorano, J., Aragón-Salamanca, A., & Rego, M. 1995, ApJ, 455, L1, astro-ph/9510061
 Giallongo, E., D'Odorico, S., Fontana, A., Cristiani, S., Egami, E., Hu, E. M., & McMahon, R. G. 1998, AJ, in press, astro-ph/9802340
 Hauser, M. G. et al. 1998, preprint
 Hu, E. M., & McMahon, R. G. 1996, Nature, 382, 231, astro-ph/9606135

- Hu, E. M., McMahon, R. G. & Egami, E. 1996, ApJ, 459, L53, astro-ph/9512165
- Hu, E. M., McMahon, R. G. & Egami, E. 1997, in *HST and the High Redshift Universe*, ed. N. R. Tanvir, A. Aragón-Salamanca, & J. V. Wall (Singapore: World Scientific), 91, astro-ph/9609188
- Kennicutt, R. C., Jr. 1983, ApJ, 272, 54
- Lowenthal, J. D. et al. 1997, ApJ, 481, 673, astro-ph/9703093
- Madau, P., Ferguson, H. C., Dickinson, M. E., Giavalisco, M., Steidel, C. C., & Fruchter, A. 1996, MNRAS, 283, 1388, astro-ph/9607172
- Madau, P., Pozzetti, L., & Dickinson, M. E. 1997, ApJ, submitted, astro-ph/9708220
- Oke, J. B. et al. 1995, PASP, 107, 375
- Pascarelle, S. M., Windhorst, R. A., Keel, W. C., & Odewahn, S. C. 1996, Nature, 383, 45
- Petitjean, P., Pécontal, E., Valls-Gabaud, D., & Charlot, S. 1996, Nature, 380, 411, astro-ph/9603088
- Pritchett, C. J. 1994, PASP, 106, 1052
- Smail, I., Ivison, R. J., & Blain, A. W. 1997, ApJ, 490, L5, astro-ph/9708135
- Songaila, A., Cowie, L. L., Hu, E. M., & Gardner, J. P. 1994, ApJS, 94, 461
- Steidel, C. C., Adelberger, K., Dickinson, M., Giavalisco, M., Pettini, M., & Kellogg, M. 1998, ApJ, 492, 428, astro-ph/9708125
- Steidel, C. C., Giavalisco, M., Dickinson, M., & Adelberger, K. L. 1996a, AJ, 112, 352, astro-ph/9604140
- Steidel, C. C., Giavalisco, M., Pettini, M., Dickinson, M., & Adelberger, K. L. 1996b, ApJ, 462, L17, astro-ph/9602024
- Storrie-Lombardi, L. J., McMahon, R. G., Irwin, M. J., & Hazard, C. 1996, ApJ, 468, 121, astro-ph/9604021
- Thommes, E. 1996, PhD thesis, Univ. Heidelberg
- Thommes, E. & Meisenheimer, K. 1995, in *Galaxies in the Young Universe*, ed. Hippelein, H., Meisenheimer, K., & Röser, H.-J. (Berlin: Springer), 242
- Thommes, E., Meisenheimer, K., Fockenbrock, R., Hippelein, H., & Röser, H.-J. 1998, MNRAS, 293, L6
- Thompson, D., Djorgovski, S., & Trauger, J. 1995, AJ, 110, 963
- Thompson, D. & Djorgovski, S. G. 1995, AJ, 110, 982

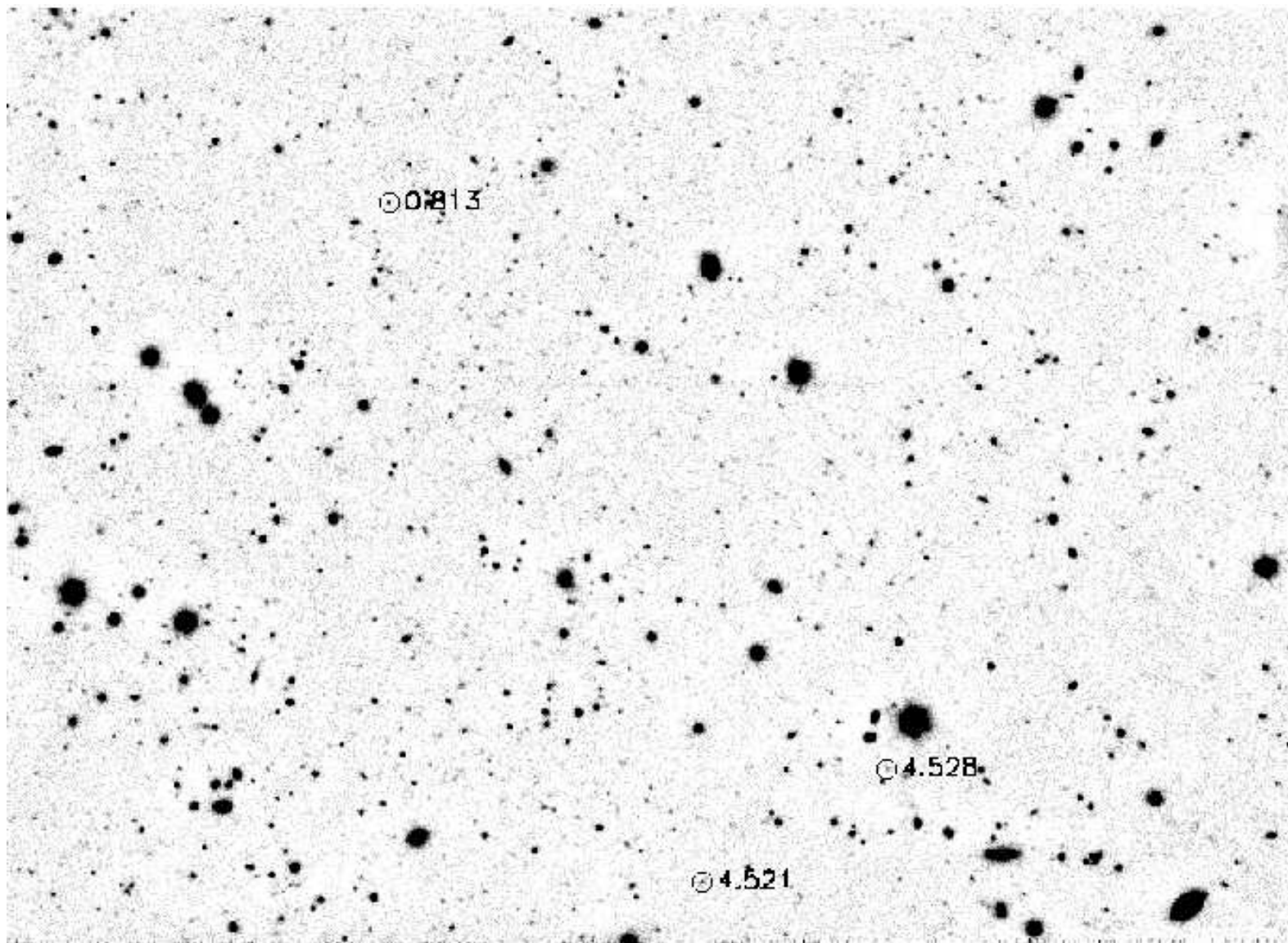


Fig. 2.— (Plate 1) A 2.7 hr Keck narrowband image of the $6' \times 4'$ region around the SSA22 field through a 78 \AA filter centered at 6741 \AA . Objects with observed equivalent widths $W_\lambda > 100 \text{ \AA}$ are circled. The object with the lowest observed equivalent width ($W_\lambda = 120 \text{ \AA}$) is spectroscopically identified as a $z = 0.813$ [O II] emitter. However, the two higher equivalent width objects appear to be $\text{Ly}\alpha$ emitters ($W_\lambda = 200 \text{ \AA}$, $z = 4.521$ and $W_\lambda = 1000 \text{ \AA}$, $z = 4.528$).

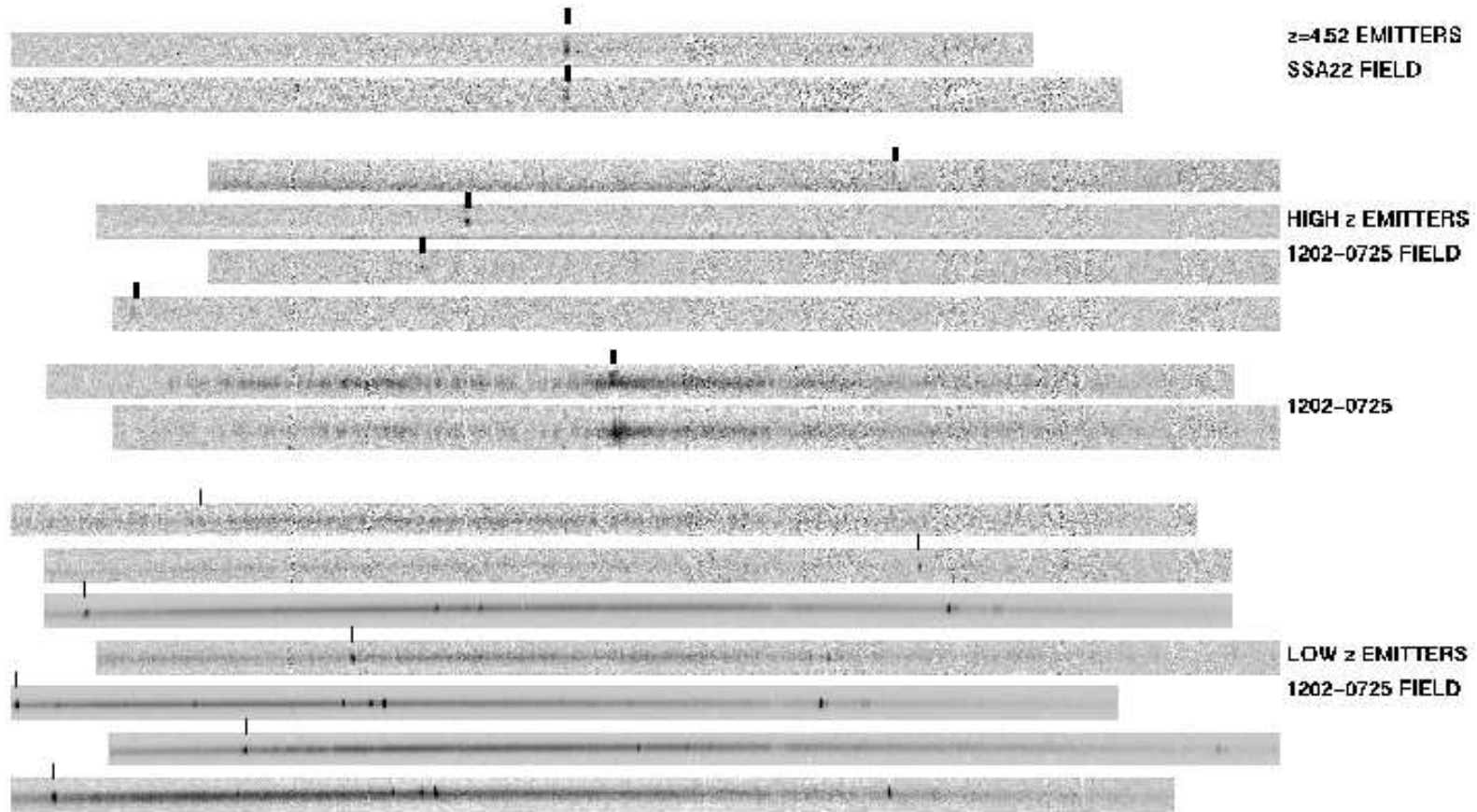


Fig. 3.— (Plate 2) Gray scale images of emission-line objects selected in the spectroscopic observation of the BR1202–0725 field and of the two emitters in the SSA22 field (Plate 1) selected in the 6741/78 Å filter (*top two panels*). The images have been registered in wavelength with a range from 4400 Å to 9700 Å. The lower seven panels show emission-line objects at $z < 1.20$ in the spectral image. For each object, the [O II] $\lambda 3727$ line is indicated. The two middle panels show the $z = 4.69$ quasar, BR1202–0725, observed at two different orientations. Narrow, spatially separated Ly α emission without strong continuum is seen at both angles, corresponding to the two companions to the quasar (Hu, McMahon, & Egami 1996; Fontana et al. 1996; Petitjean et al. 1996; Hu, McMahon, & Egami 1997). The next four panels show the single emission-line objects (*thick tick marks*) in the BR1202–0725 field. The two longer wavelength objects at $z = 4.19$ and $z = 5.64$ have continuum breaks across the emission line of $2.3^{+2.6}_{-2.0}$ and $2.6^{+5.2}_{-1.8}$ respectively, suggesting that this line is Ly α , while the two lower wavelength lines, where no continuum is visible, have none of the additional emission lines which would be seen if they were at lower redshift. (The longest wavelength emission line object lies close to a bright foreground galaxy at $z = 0.236$, whose spectrum can be seen at the bottom edge of the image. However, the required velocity separation of -1500 km s^{-1} would seem large for the line to be interpreted as H α from an extragalactic HII region associated with this object.) For the SSA22 ($z \sim 4.52$) objects, the spectrum in the upper panel shows a continuum break, while the lower panel’s spectrum is only an isolated emission line.